JOURNAL OF APPLIED POLYMER SCIENCE VOL. 15, PP. 1623–1639 (1971)

The Size Analysis of Polymer Latices by Electron Microscopy Using Freeze-Etched Preparations

R. REED and J. R. BARLOW, *The Procter Department of Food and Leather Science, The University, Leeds, England*

Synopsis

A range of styrene–butyl acrylate copolymer latices has been studied in the electron microscope, using the freeze-etching method of specimen preparation. This involves the rapid freezing of a small specimen, fracture of the frozen block, followed by replication of the fracture surface. The process of freezing rapidly to liquid air temperatures minimizes deformation of "soft" latex particles and allows their size to be determined. Certain latices were also investigated using a conventional method of specimen preparation, involving size measurements on dried, deformed particles. The particles observed in freeze-etched preparations appeared to have slightly smaller diameters.

INTRODUCTION

Among the methods available for latex particle size determination, electron microscopy alone allows visual inspection of the individual particles. However, particles of film forming, or so-called "soft" latices, deform somewhat during the drying stage of their preparation so that it is difficult to estimate their size directly. Several techniques have been introduced to overcome this difficulty including:

1. Bromination of the particles to induce "hardening," so that their deformation on drying is reduced.[1–3] The contrast of the preparation is also enhanced. For certain types of latex this method is most satisfactory, but it is based on residual unsaturation in the polymer system, which in certain cases, e.g., acrylates, may be absent.
2. "Hardening" the particles by irradiation with high-energy electrons, to bring about crosslink formation.[4] The two disadvantages of this method are (a) electrons of extremely high energy are needed and (b) certain polymer systems are degraded rather than hardened. A refinement of this technique is to include a small quantity of styrene monomer into the system of latex particles and bring about polymerization, with consequent "hardening," by irradiation with electrons of much lower energy.[5]
3. Staining the particles with solutions of uranyl acetate, thereby increasing the contrast and allowing easier measurement of their size.[6] When using this method, no corrections are normally made for any deformation which might occur on drying the specimen.

4. Embedding the soft particles in a polymeric film of different density, thereby physically fixing the particles and preventing their deformation.[7] This method, however, does not lead to any increase in specimen contrast, so that size determination may still be difficult.

5. Measurement of the parameters of the deformed particles produced on drying a soft latex, and calculation of the equivalent sphere diameter assuming that the deformed particles are present as segments of a sphere or as oblate spheroids.[8]

Methods 1 to 3 involve chemical modification of the particles, which could lead to changes in the conformation of the polymer chains. The overall size of each particle, therefore, may have been altered by an appreciable, but indeterminate, amount. The change in size following bromination has been measured in several cases,[16] and it depends on the particular polymer studied. However, where the size distribution rather than the mean diameter is required, the effects of chemical treatment will be of less importance.

All the methods outlined above involve placing the polymer particles directly in the electron beam, with the risk of damage by the latter.[8] The damage to soft particles may be quite considerable, for even polystyrene particles, which are extremely "hard" (and often used for magnification calibration), may expand, or even melt, under the action of the electron beam. To minimize the effects of electron beam damage, the specimens are often mounted on stainless steel grids, rather than the more usual copper type.

Any method, therefore, which minimizes the chemical modification of the latex particles and avoids the possibility of electron beam damage is likely to be most useful. The method of freeze etching goes a long way to meet these conditions, since the specimen is fixed by freezing and yields a stable metal/carbon replica of a fracture surface in the frozen latex.

This technique, devised by Steere[9] and developed by Moor et al.,[10] involves freezing the specimen, at rates of the order of 100°C/sec, to liquid air temperatures, thereby physically fixing the structures which are present. However, to prevent the formation of small ice crystals which might be released during freezing and would obliterate the fine details in the specimen, a cryoprotective, such as 20% aqueous glycerol, needs to be included in the sample. The frozen latex droplet is fractured with a cooled knife and the fracture surface thus exposed is shadow cast with platinum/carbon. The replica film is then reinforced with a thin layer of vertically deposited carbon, isolated by dissolving away any remaining latex, and finally examined.

Experience with freeze-etched preparations is at present rather limited, and mostly it has been confined to the biologic field.[11–14]

EXPERIMENTAL

Preparation of Latices. These were prepared by Mr. A. G. Marriott, British Leather Manufacturers' Research Association, Egham, Surrey, and their chemical compositions are shown in Table I.

The polymers were prepared as 25% Total Solids emulsions using 3.0% w/w lauryl sulfate as surfactant and ammonium persulfate as initiator (2.0

TABLE I
Latex Properties

Latex no.	Styrene in monomer charge, %	Butyl acrylate in monomer charge, %	Conversion at completion, %	T_g, °C
1	100	0	89.5	+108°C
2	80	20	87.0	+33°C
3	50	50	92.0	+25°C
4	20	80	93.5	−33°C
5	10	90	99.0	−38°C
6	5	95	98.0	−47°C
7	0	100	99.0	−50°C

$\times 10^{-4}$ moles/moles of monomer). The reaction was carried out under self-sustaining reflux at 80°C for 10 min and under forced reflux at 96°C.

Freeze Etching. The commercial form of Moor's apparatus, as supplied by Messrs. Balzers AG, Lichtenstein, was employed. A small sample of latex was diluted with a quarter of its own volume of glycerol and gently agitated to ensure complete dispersion. A small droplet of the mixture was placed in the central cavity of a 3-mm gold disc by means of a micropipet, the mounted specimen then being rapidly frozen by immersion in a liquid refrigerant (Arcton 22) maintained at −150°C. The specimen was transferred to liquid nitrogen after 5 sec and stored until required. The table of the freeze-etch apparatus was cooled to −150°C and coated with liquid refrigerant prior to the transfer of the mounted specimen from the storage vessel. Having placed the specimen in position on the work table, a vacuum was drawn on the system and the temperature of the specimen was raised to −100°C. When a vacuum better than 10^{-6} torr had been established, planing of the sample with a microtome knife, cooled to −196°C, was carried out. Etching, or differential removal of ice from the sample surface to reveal structural details, was carried out for 90 sec, the cooled microtome knife being held 1 mm above the specimen. The etched surface was then shadow cast with platinum/carbon, and the replica thus formed was reinforced by the vertical deposition of a thin carbon layer. The specimen was removed from the work chamber, allowed to thaw, and placed in a solvent (toluene/alcohol mixture) to dissolve away the remaining latex. The replica film was isolated, taken through an alcohol/water series, and finally washed on the surface of distilled water. After mounting the replica on a copper grid, examination was carried out in an A.E.I. EM6B electron microscope.

Conventional Preparation Technique. The softest latex was diluted to approximately 200 ppm polymer and sprayed on a grid coated with a carbon/collodion film. After drying, a polystyrene latex also containing approximately 200 ppm solids was sprayed on to the grid. After drying the specimen was shadow cast with chromium. The method was repeated using latex 1 alone.

RESULTS

All plates are negative prints and, unless otherwise stated, the scale mark represents 200 nm.

Freeze-Etch Preparations

Figure 1 is a low-magnification view of a typical replica produced by the freeze-etch method. The distinction between areas subjected to fracture of the specimen and those across which the microtome has simply cut is immediately apparent. The grooves in the cut areas are known as "knife marks" and indicate the direction of the knife movement. In such areas there is a lack of detail and contrast, and hence the study of micrographs from freeze-etch preparations is restricted to the areas of true fracture.

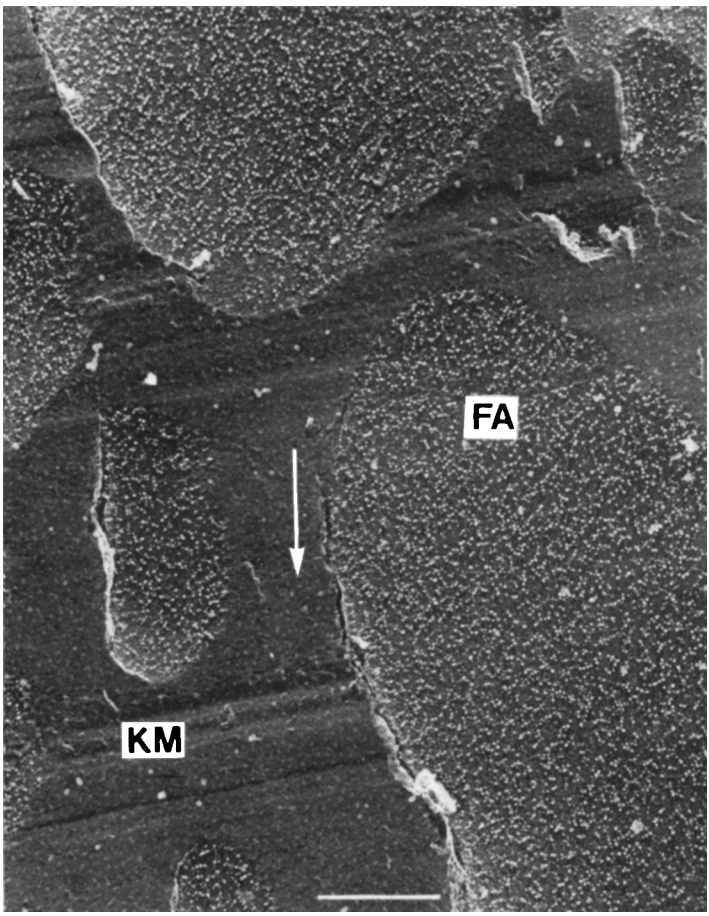

Fig. 1. Low-magnification view of a typical freeze-etch replica. Shadowing direction indicated by arrow. FA = Fracture area; KM = knife marks. Scale mark 2 μm.

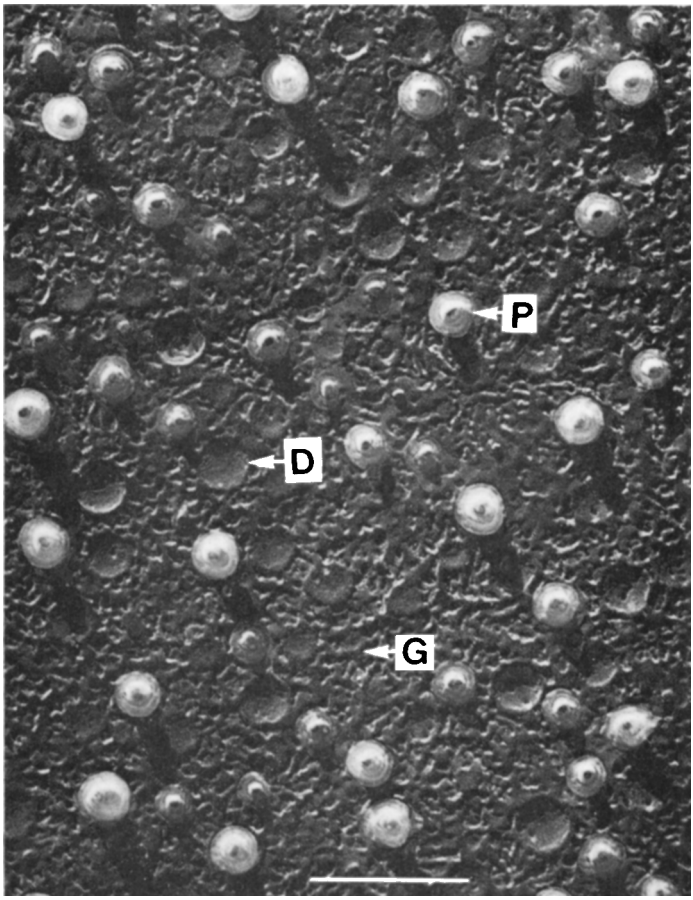

Fig. 2. High-magnification view of a fracture area in a freeze-etch preparation of latex 1. P = Protrusion, containing residual polymer; D = depression; G = ground substance, or ice matrix.

The unequivocal direction of shadowing is readily seen, demonstrating that the fracture process involves the removal of scoops of material from the specimen by the microtome knife. In freeze-etch preparations, it is often difficult to distinguish between protrusions and depressions unless the shadowing direction is known with certainty, since both formations yield images composed of dark and light areas.

The individual polymer particles protruding from the fracture surface of the replica film are visible as white dots in the micrographs. Such protrusions are opaque in the electron beam since the solvent has failed to enter the small fissures in the replica, and the polymer consequently remains.

Figure 2 is a higher-magnification view of the fracture surface produced by knife action on latex 1, which consists of polystyrene alone. The protrusions, formed by the fracture surface passing over a polymer particle embedded in the frozen matrix, and the depressions, produced by a latex par-

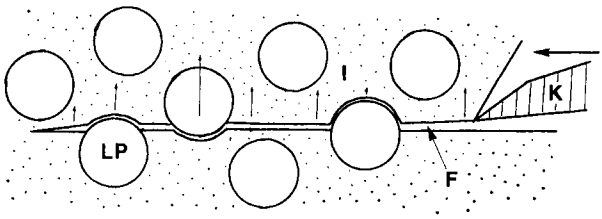

(a)

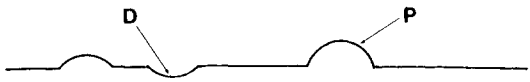

(b)

Fig. 3. Diagrammatic representation of knife action on a frozen latex specimen. (a) Fracture mechanism: LP = latex particle; I = ice matrix; K = knife; F = fracture plane extending in front of knife; heavy arrow = direction of knife movement. (b) Metal/carbon replica of the fracture surface produced: D = depression; P = protrusion.

ticle being lifted out, are readily distinguishable. It is significant that no fractured particles are observed, indicating that the polymer system is stronger than the frozen matrix. Thus, Figure 3 is probably a good representation of the process of fracture.

All particles appear spheroidal, but the lack of deformation is to be expected, as polystyrene particles are traditionally considered "hard." The uneven nature of the frozen matrix material is indicative of the presence of salts, soaps, or emulsifiers in the latex composition.

Figure 4 is a freeze-etched view of latex 3, in which a considerable amount of butyl acrylate was copolymerized with styrene. There appears to be no significant change in the appearance of the specimen; in other words, the introduction of butyl acrylate has not softened the polymer particles as visualized by this technique.

Figure 5 shows latex 7, composed of poly(butyl acrylate), prepared by freeze etching. Again there are no distinguishing features to set this specimen apart from earlier examples, for all paricles appear spheroidal and all depressions are equally distinct. Thus, it is possible to obtain information for all the latices studied, since they all appear to freeze satisfactorily.

Since all protrusions in the replicas contained residual polymer that had not been removed by solvent treatment, it was decided to measure and to

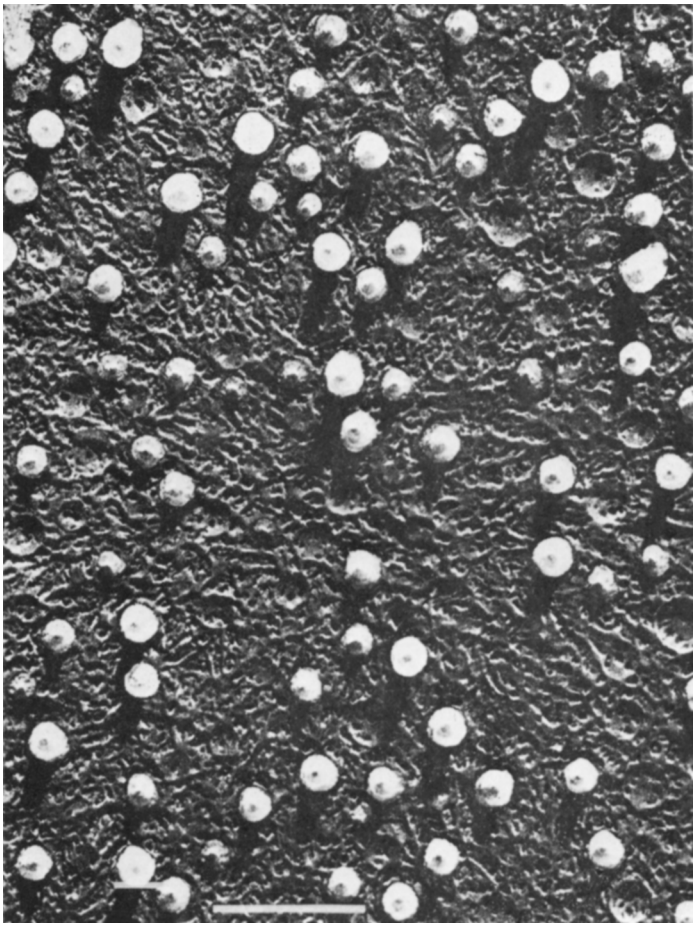

Fig. 4. High-magnification view of a fracture area in a freeze-etch preparation of latex 3.

count the depressions on each micrograph. The histograms resulting from such counts are shown in Figure 6.

Conventionally Prepared Specimens

Latex 1, when prepared for electron microscope investigation by a dilution-plus-drying technique, yielded micrographs such as Figure 7. The large number of very small particles, which do not appear in freeze-etched preparations, is immediately apparent. Comparison with the micrographs obtained by Davidson and Collins[15] indicates that emulsifier soaps may be responsible for the appearance of such small particles. (The appearance of discrete structures due to soap separation is not expected in freeze-etched preparations, since the process of freezing will keep all emulsifiers and soaps in solution and lead to the observed uneven nature of the fractured frozen matrix.)

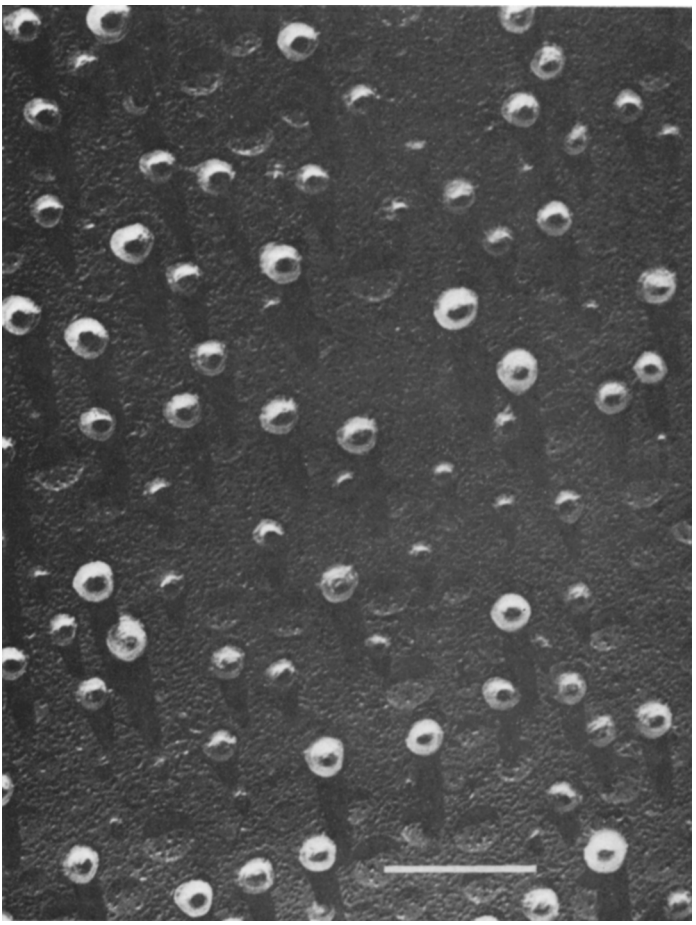

Fig. 5. High-magnification view of a fracture area in a freeze-etch preparation of latex 7.

Close inspection of the polystyrene latex shows that each particle is surrounded by a halo or fringe. This effect was observed even when great care was taken to photograph the specimen as quickly as possible while using the cold-finger anticontamination device on the electron microscope. Such halos are not generally found with polystyrene and presumably are peculiar to this particular sample. The electron beam may cause the particles to soften and expand, thereby bringing considerable inaccuracy into the results of size determination obtained by this method of specimen preparation.

The histogram obtained by counting the particles and measuring their diameters is shown in Figure 8. The mean particle diameter was found to be 66 nm.

Figure 9 shows both hard and soft particles (from latices 1 and 7, respectively) present in the same field. The marked deformation of the soft particles is demonstrated by the low height-to-width ratio (approximately 0.1), as calculated from the shadowing angle. The calculation method of

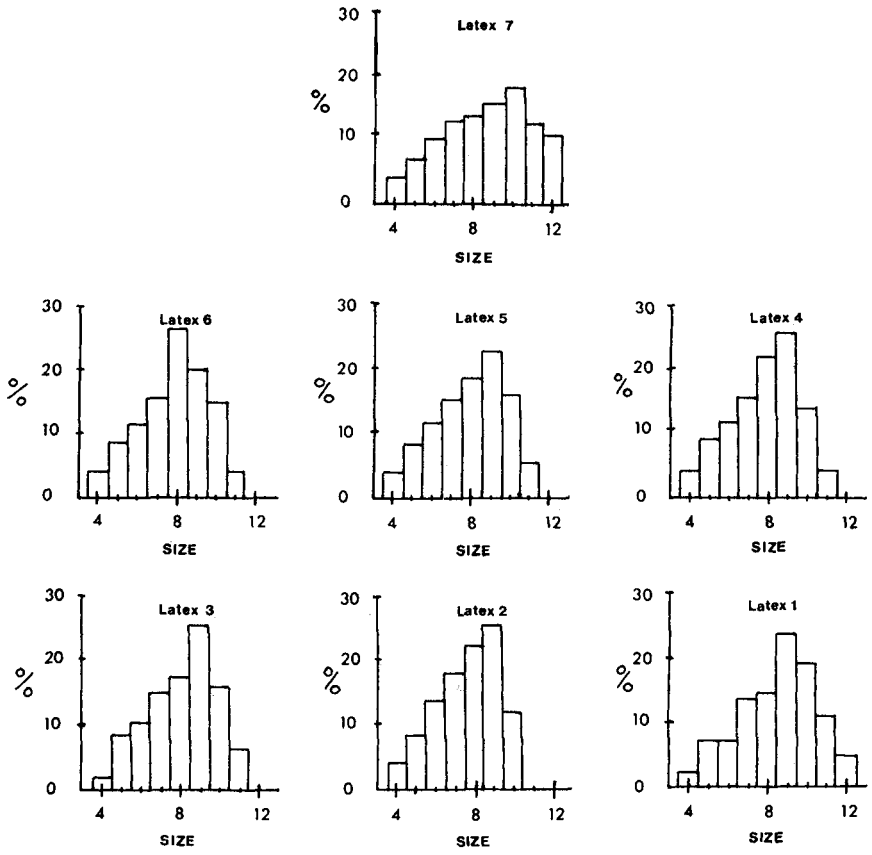

Fig. 6. Depression diameter histograms for latices 1 to 7, from direct measurements on micrographs of freeze-etch preparations, at a magnification of 170,000×. Sizes correspond to millimeters on the micrographs.

Bradford and Vanderhoff[8] was applied, and for the soft latex a mean particle diameter of 75 nm was obtained.

THEORY

The size of the depressions and protrusions in the replica film may be used for particle size analysis. However, since the depth of a depression, or height of a protrusion, cannot be directly measured, the level at which the fracture surface passes round each latex particle is not known. As shown in Figure 10, the true size of a particle cannot be obtained directly from measurements taken on the replica film, and hence a distinction between true and observed diameters is necessary. The particle sizes which are measured, therefore, need to be corrected to take this effect into account.

The assumptions used in the theoretical treatment are: (1) The latex particles are spherical. (2) The level at which a particle is exposed is deter-

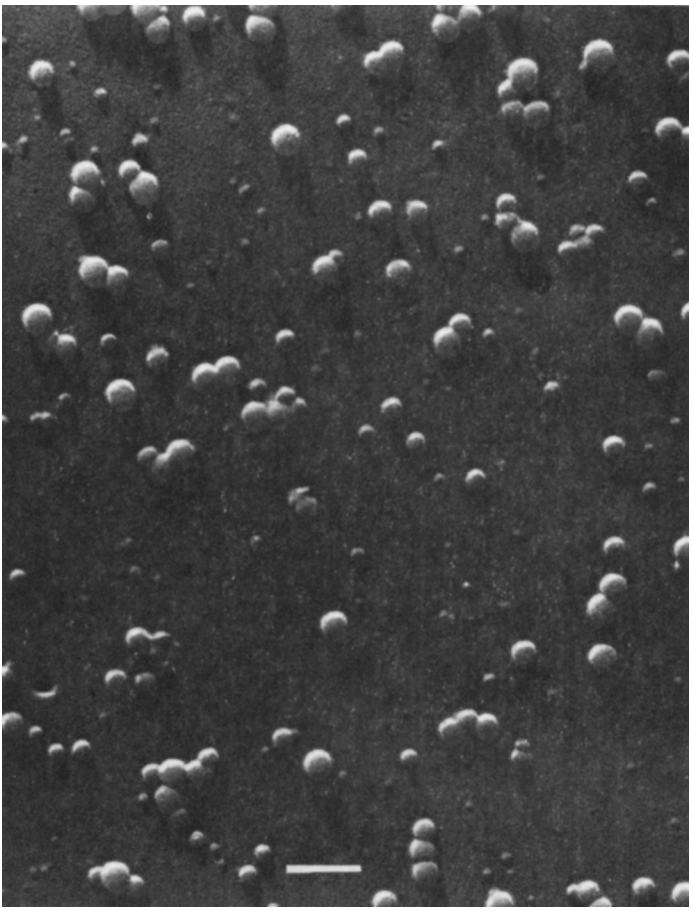

Fig. 7. Latex 1, after dilution, spraying, and drying.

mined solely by its position within the frozen matrix, while there is also a regular distribution of particles in a vertical direction within the specimen. (3) The largest observed depressions (or protrusions) arise from exposure about the "equatorial" regions of the largest particles in the latex.

Let the depressions in a micrograph of a freeze-etched latex sample be sized and counted (the theoretical considerations for protrusion measurements are exactly the same). The results are tabulated in the form of a histogram with mean class diameters X_1, X_2, X_3 . . . , X_n, the boundary limits between these histogram classes being a_1, a_2, a_3 . . . , a_n. (see Fig. 11a). Let the fraction of the total number of particles in each histogram class also be calculated.

If a particle with true diameter X_1 is considered, it is clear that the *observed* diameter of the depression, produced on removal of the particle from the frozen matrix, will depend on the level at which the fracture plane passed around the particle.

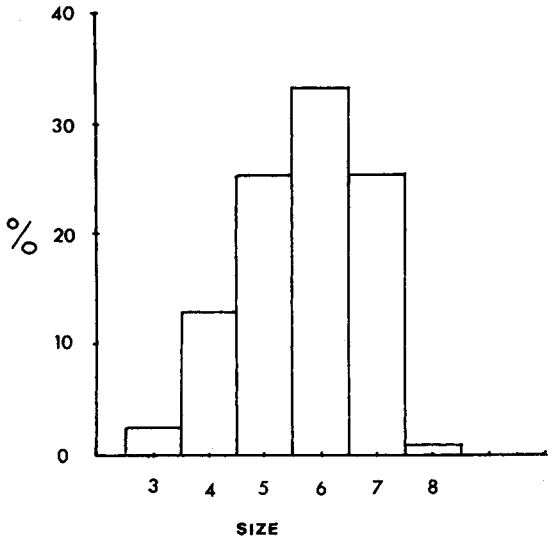

Fig. 8. Particle size measurements of latex 1, prepared by a conventional dilution plus drying technique, from micrographs at 85,000×.

If the fracture plane lies between levels 1 and 2 (see Fig. 11a), the exposed depression will have an *observed* diameter between X_1 and a_1; hence it will be recorded in the X_1 histogram class. However, if the fracture plane lies between levels 2 and 3, the exposed depression will have an observed diameter between a_1 and a_2, and hence it will be recorded in the X_2 histogram class. Similarly, further levels may be drawn corresponding to observation of the particle in histogram classes $X_3, X_4, \ldots, X_n$.

Since a regular distribution of the particles with respect to the vertical axis has been postulated, the chance of a particle with true X_1 giving a depression of observed diameter X_1 is proportional to y_1, the vertical distance between the two a-value extremes of the histogram class. Similarly, the chance of a particle with true diameter X_1 giving a depression of observed diameter X_2 is proportional to y_2. This reasoning may be applied to find the relative probabilities for particles having a true diameter of X_1 appearing in all the histogram classes.

Thus, the fraction of all particles having a true diameter of X_1 giving a depression of observed diameter X_1 is equal to $y_1/\sum_{i=1}^{i=n} y_i$ and the fraction of such particles giving depressions of observed diameter X_2 is $y_2/\sum_{i=1}^{i=n} y_i$. If the assumption is made that even the smallest depressions are observed and counted, then

$$\sum_{i=1}^{i=n} y_i = \frac{X_1}{2}.$$

However, if this is not the case, the denominator must be calculated from the results obtained.

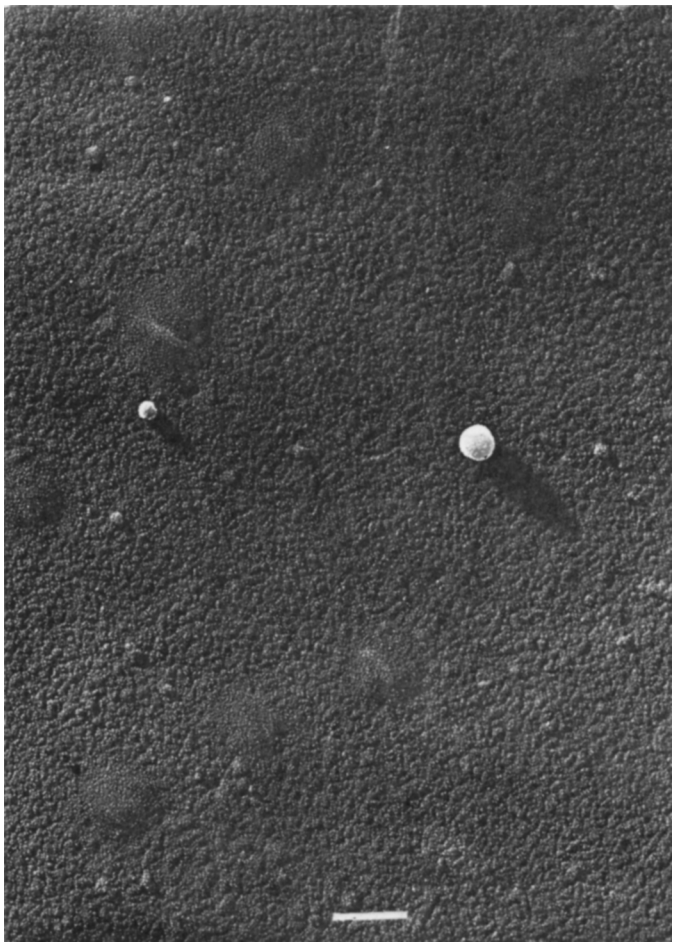

Fig. 9. Latices 1 and 7, after dilution, spraying, and drying.

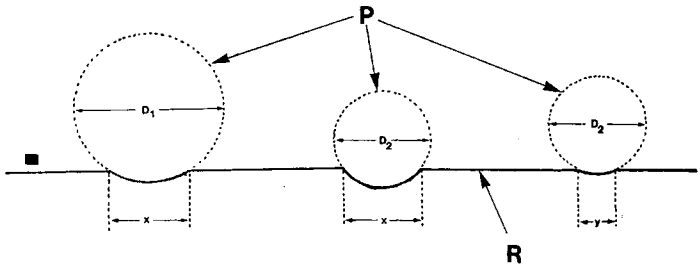

Fig. 10. Showing the effect of fracture level on observed depression diameter; $D_2 > D_1$ but both particles give depressions of the same diameter, x, in the replica. R = Replica; P = original particles giving depressions in replica.

Considering now all particles having a true diameter X_2, and applying the same arguments as outlined above, it is possible to determine the distribution of such particles in the various histogram classes (see Fig. 11b). The fraction of particles having a true diameter of X_2 giving a depression with observed diameter X_2 is equal to $y_1'/\sum_{i=1}^{i=n} y_i'$. Similar expressions are obtained to find the fraction of the number of particles having a true diameter of X_2 which appear in each histogram class. Similar calculations are applied in turn to particles having true diameters X_3, X_4, ..., X_n to find their number distributions among the histogram classes.

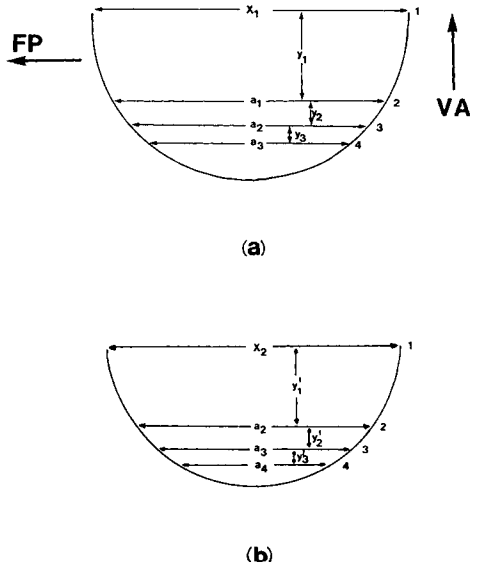

Fig. 11(a). Showing the observed depression diameter as a function of fracture level, in particles with a true diameter of X_1. (b). Showing the observed depression diameter as a function of fracture level, in particles with a true diameter of X_2. VA = Vertical axis; FP = fracture plane direction.

From simple geometry and from substitution of the measured values of $X_1, X_2, X_3, \ldots, X_n$ (which automatically define the values $a_1, a_2, \ldots, a_n$), all coefficients of the form $y/\sum y$ can be calculated. The set of coefficients used for the latices studied is shown in Table II, the units being the depression diameters, measured on the micrograph, in mm. Now, the fraction of the total number of depressions having an observed diameter of X_1 is equal to $\left[y_1/\sum_{i=1}^{i=n} y_i \right] \times A$ when A is the number of particles having a true diameter X_1 divided by the total number of particles. Since the coefficient $y_1/\sum_{i=1}^{i=n} y_1$ has been calculated, comparison of the observed and calculated values allows A to be found.

TABLE II
True Diameter–Observed Diameter Correlation Coefficients

	12	0.03	0.04	0.05	0.06	0.07	0.10	0.13	0.22	0.30
↑	11	0.04	0.05	0.06	0.08	0.10	0.14	0.22	0.31	
True	10	0.05	0.06	0.08	0.11	0.15	0.23	0.33		
diameter	9	0.06	0.08	0.11	0.15	0.23	0.35			
(mm on	8	0.08	0.10	0.18	0.26	0.38		$\frac{y}{\Sigma y}$		
print)	7	0.12	0.17	0.29	0.42				values	
	6	0.18	0.33	0.49						
	5	0.39	0.61							
	4	1.00								
		4	5	6	7	8	9	10	11	12

Observed diameter →
(mm on print)

The fraction of the total number of depressions having an observed diameter of X_2 is equal to

$$\left[\frac{y_2}{\sum_{i=1}^{i=n} y_i} \times A\right] + \left[\frac{y_1'}{\sum_{i=1}^{i=n} y_i'} \times B\right]$$

where B is the number of particles with a true diameter X_2 divided by the total number of particles. The two factors in the expression arise since particles having a true diameter of either X_1 or X_2 may give depressions with an observed diameter X_2. Comparison of observed and calculated results, together with the substitution for A found previously, enables B to be calculated.

This process is repeated for particles giving depressions with observed diameters X_3, X_4, ..., X_n; and relevant substitution of known values, together with comparison of observed and calculated results, enables the true number of particles in each histogram class to be calculated and later used in mean particle size determinations.

DISCUSSION

As a preparative method, freeze etching certainly appears useful for examining latices covering a wide range of chemical compositions and physical properties, without the need for radical chemical alteration of the specimen. However, as with all new techniques, caution is needed when interpreting the information from freeze-etch micrographs, since the possibility of physical modification remains. For example, the effects of "deep freezing" a latex are not completely known. The rate of freezing is so rapid that no appreciable deformation of the particles can occur, but the accompanying volume changes may be quite considerable. Although the polymer itself may have a very low coefficient of thermal expansion or contraction, the surrounding aqueous phase may exert strong forces on the latex particles during freezing. The addition of glycerol, to prevent the release of ice crystals

during the freezing stage, could possibly affect the results obtained from the freeze-etch method. In fact, ice crystal formation is not observed when these particular latices are frozen in the absence of glycerol, but all the particles coalesce into large clumps that cannot be satisfactorily resolved. Thus, the glycerol appears to prevent aggregation during freezing, but its presence should only be detrimental if the solubility of polymer in glycerol is appreciable.

The measurement of depression diameters indicates that the fracture plane mostly lies normally to the plane of viewing to give circular depressions and for the theoretical treatment to be valid. From the low-magnification view of a freeze-etch replica, however, it is obvious that the orientation of the fracture plane varies across each "scoop" of removed material. Thus, if the fracture plane is not perfectly horizontal relative to the vertical direction in which the replica is viewed, the depressions formed on removal of latex particles will not appear circular, but rather ellipsoidal. However, such depressions may still yield accurate results provided that the major axis of each ellipse is measured and used in the results, since this parameter will be unaffected by fracture plane orientation and will always equal the "diameter" of the depression.

The advantages of the freeze-etch method of specimen preparation are many, but the avoidance of radical chemical alteration of the latex particles is obviously most important. If the structure and composition of the polymer remain unchanged during specimen preparation, a possible major source of error in quantitative measurements is removed. A further feature is that the specimen to be studied in the electron microscope is not composed of a polymer liable to electron beam damage and subsequent deformation, but of a platinum/carbon replica film. Thus, no special precautions such as very rapid focussing or high energy electrons need be employed, while all measures to improve resolution, contrast, and focussing may be fully exploited.

The correction of observed results to yield true particle size distributions is very simple and quick, once $y/\sum y$ coefficient tables have been constructed. Also important in this connection is the large number of particles appearing in the same field, so that relatively few micrographs are needed to give a statistically significant particle size distribution. It may be also noted that, given a specimen of slightly larger particle size, it is possible to study surface details on each latex particle, a task which is difficult by any other method. The extremely small size of the particles used in the present work meant that surface details were beyond the limits of resolution afforded by a shadowed replica technique.

Thus, various factors may determine the results obtained from freeze-etch preparations, and the extent to which these are operative may be gauged from Figure 12, showing particle size histograms after applying the theoretical correction. Comparison with Figure 6, in which the corresponding uncorrected results are presented, shows that all small depressions arise from the removal of large particles from the frozen matrix, rather than from fracture across the equatorial regions of small particles.

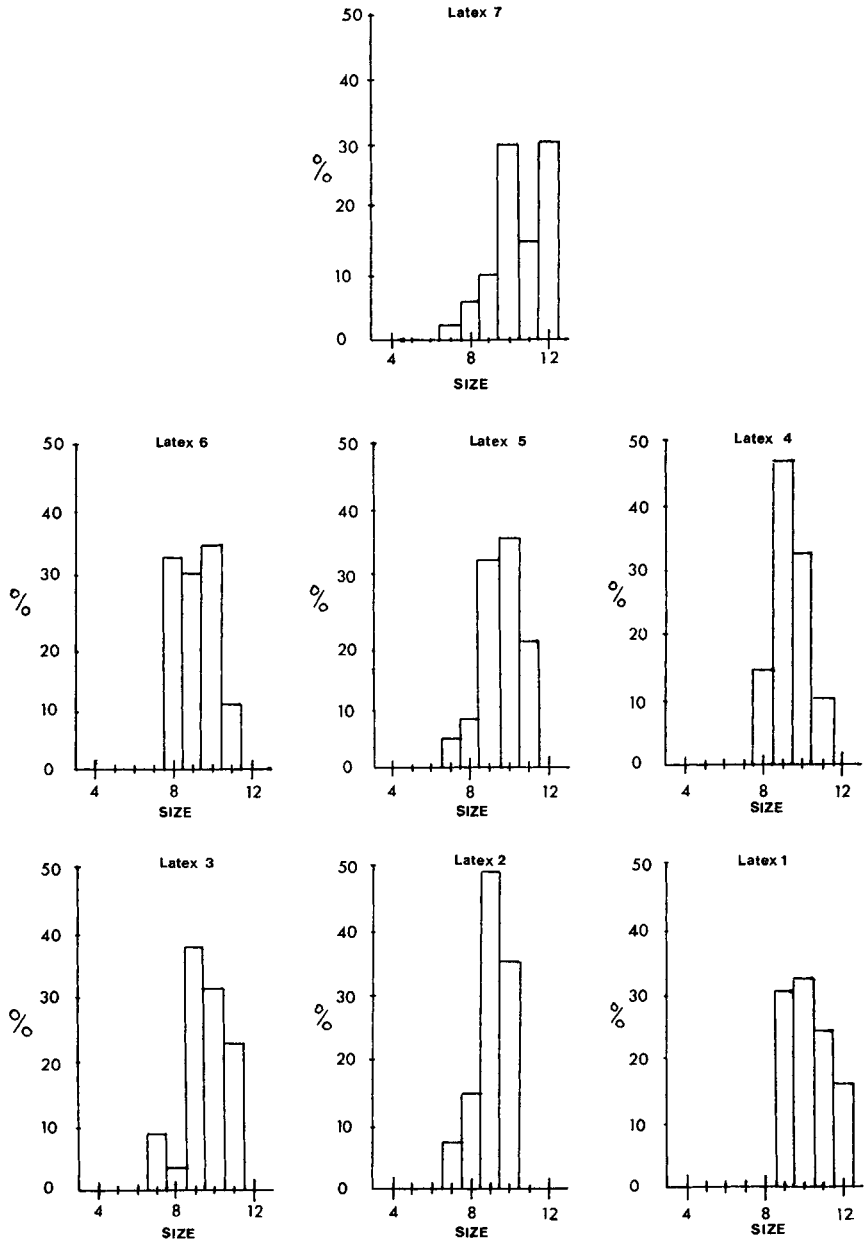

Fig. 12. Corrected particle size counts of latices 1 to 7, from micrographs of freeze-etched preparations at 170,000× (sizes in millimeters).

Perhaps the most striking feature of the results is that the size distributions of the latex particles as obtained from freeze-etch preparations differ from those normally obtained by other, well-established techniques in that asymmetry occurs. In the present study, about 600 particles were counted for

TABLE III
Particle Counts and Sizes

Latex no.	Number of particles counted	Mean depression diameter, nm	Mean particle diameter, nm
1	620	50	55
2	580	47	53
3	580	46	52
4	560	46	55
5	550	47	56
6	620	46	54
7	620	51	61

each latex (see Table III), but to obtain more precise information regarding size distribution, larger numbers would perhaps be required.

As calculated from Figure 12, the mean particle sizes of latices 1 and 7 were found to be 60 and 61 nm, respectively, or 8% and 20% lower than the corresponding values obtained from dried, diluted specimens. It is difficult to say, however, whether these differences arise during the preparation of freeze-etched specimens or from electron beam damage to the dried specimens prepared by conventional techniques. Thus, although freeze etching can yield acceptable micrographs of "soft" latices, further work is needed before the quantitative measurements obtained from its use can be accepted as accurate. However, the versatility of the method is beyond question, and important qualitative applications may be expected.

References

1. W. E. Brown, *J. Appl. Phys.*, **18**, 273 (1947).
2. E. A. Willson, J. R. Miller, and E. H. Rowe, *J. Phys. Colloid Chem.*, **53**, 357 (1949).
3. S. H. Maron, C. Moore, and A. S. Powell, *J. Appl. Phys.*, **23**, 900 (1952).
4. E. B. Bradford and J. W. Vanderhoff, *J. Colloid Sci.*, **14**, 543 (1959).
5. E. Vanzo, R. H. Marchessault, and V. Stannett, *J. Colloid Sci.*, **19**, 578 (1964).
6. G. Hebestreit, G. Reich, and F. Stather, *Das Leder*, **17**, 227 (1966).
7. R. H. Kelsey and E. E. Hansen, *J. Appl. Phys.*, **17**, 675 (1946).
8. E. B. Bradford and J. W. Vanderhoff, *J. Colloid Sci.*, **17**, 668 (1962).
9. R. L. Sterre, *J. Biophys. Biochem. Cytol.*, **3**, 45 (1957).
10. H. Moor, K. Mühlethaler, H. Waldner, and A. Frey-Wyssling, *J. Biophys. Biochem. Cytol.*, **10**, 1 (1961).
11. H. Moor, *J. Appl. Phys.*, **35**, 3099 (1964).
12. A. Frey-Wyssling, *Advan. Sci.*, 109 (July, 1966).
13. R. Reed, J. S. Kennelly, and I. D. Boyes, *J. Soc. Leather Trades Chem.*, **52**, 257 (1968).
14. R. Reed and P. J. Rothwell, *Brit. J. Derm.*, **82**, 470 (1970).
15. J. A. Davidson and E. A. Collins, *J. Colloid Interfac. Sci.*, **24**, 456 (1969).
16. Z. Pelzbauer, V. Hynkova, M. Bezdek, and F. Hrabak, *J. Polym. Sci. C*, **16**, 503 (1967).

Received October 10, 1970